



Equatorward phytoplankton migration during a cold spell within the Late Cretaceous supergreenhouse

5 Niels A.G.M. van Helmond^{1*}, Appy Sluijs¹, Nina M. Papadomanolaki¹, A. Guy Plint²,
Darren R. Gröcke³, Martin A. Pearce⁴, James S. Eldrett⁵, João Trabucho-Alexandre^{3,6},
Ireneusz Walaszczyk⁷, Bas van de Schootbrugge¹, Henk Brinkhuis^{1,8}

¹Marine Palynology and Paleocyanography, Laboratory of Palaeobotany and Palynology, Department of Earth Sciences, Faculty of Geosciences, Utrecht University, Heidelberglaan 2, 3584 CS Utrecht, Netherlands.

10 ²Department of Earth Sciences, The University of Western Ontario, London, Ontario, N6A 5B7, Canada.

³Department of Earth Sciences, Durham University, South Road, Durham DH1 3LE, UK.

⁴Evolution Applied Ltd, 50 Mitchell Way, Upper Rissington, Cheltenham, Gloucestershire, GL54 2PL, UK.

15 ⁵Shell International Exploration and Production Inc., Kesslerpark 1, 2288 GS Rijswijk, Netherlands.

⁶Comparative Sedimentology Group, Department of Earth Sciences, Faculty of Geosciences, Utrecht University, Heidelberglaan 2, 3584 CS Utrecht, Netherlands.

⁷Institute of Geology, Faculty of Geology, University of Warsaw, Zwirki i Wigury 93, PL-02-089 Warsaw, Poland.

20 ⁸NIOZ, Royal Netherlands Institute for Sea Research, P.O. Box 59, 1790 AB Den Burg, Texel, Netherlands.

Correspondence to: Niels A.G.M. van Helmond (n.vanhelmond@uu.nl)

Abstract. Oceanic Anoxic Event 2 (OAE2), a ~600 kyr episode close to the Cenomanian-Turonian boundary (ca. 94 Ma), is characterized by widespread marine anoxia and ranks amongst the warmest intervals of the Phanerozoic. The early stages of OAE2 are, however, marked by an episode of widespread transient cooling and bottom water oxygenation: the Plenus Cold Event. This cold spell has been linked to a decline in atmospheric $p\text{CO}_2$, resulting from enhanced global organic carbon burial. To investigate the response of phytoplankton to this marked and rapid climate shift we examined the biogeographical response of dinoflagellates to the Plenus Cold Event. Our study is based on a newly generated geochemical and palynological dataset from a high-latitude Northern Hemisphere site, Pratts Landing (western Alberta, Canada). We combine this data with a semi-quantitative global compilation of the stratigraphic distribution of dinoflagellate cyst taxa. The data show that dinoflagellate cysts grouped in the *Cyclonephelium compactum-membraniphorum* morphological plexus migrated from high- to mid-latitudes during the Plenus Cold Event, making it the sole widely found (micro)fossil to mark this cold spell. In addition to earlier reports from regional metazoan migrations during the Plenus Cold Event, our findings illustrate the effect of rapid climate change on the global biogeographical dispersion of phytoplankton.

1. Introduction

40 The Cenomanian–Turonian boundary interval (ca. 94 Ma) was an episode of extreme warmth, with tropical and mid-latitude sea surface temperatures exceeding 35 °C (e.g., Huber et al., 2002; Forster et al., 2007; Van Helmond et al. 2014a) and subtropical conditions at high latitudes (e.g., Jenkyns et al.



2004). This interval corresponds to an Oceanic Anoxic Event (OAE2), during which an increase in the production of organic carbon and a reduction in the oxygen content of seawater resulted in unusually high organic matter content of marine sediments (e.g., Schlanger and Jenkyns, 1976; Jenkyns, 2010). The OAE2 interval is stratigraphically marked by a positive carbon isotope excursion in all active carbon reservoirs, resulting from elevated organic carbon burial rates (e.g., Tsikos et al., 2004).

The early stages of OAE2 are characterized by a short-lived (ca. 40 kyr; Jarvis et al., 2011) colder interval as recorded in several marine paleotemperature records (e.g., Gale and Christensen, 1996; Forster et al., 2007; Sinninghe Damsté et al., 2010). It was first recognized as the co-occurrence of Boreal fauna with a positive oxygen isotope excursion of about 1.5‰, recorded in biogenic calcite from Beds 4–8 of the Plenus Marl in mid-latitude shelf sites of northwest Europe (Gale and Christensen, 1996). This interval was termed the ‘Plenus Cold Event’ (PCE; Fig. 1), after the Boreal belemnite *Praeactinocamax plenus* (Blainville). Subsequently, the PCE was restricted only to Bed 4 of the Plenus Marl, being the sole bed containing abundant Boreal fauna (Voigt et al., 2006; Fig. 1). Bed 4 corresponds precisely to the upper trough and second build-up of the carbon isotope excursion, the upper part of the *Metoicoceras geslinianum* ammonite Zone and basal *Whiteinella archaeocretacea* planktonic foraminifer Zone (Gale et al., 2005). More recently, Jarvis et al. (2011) extended the PCE down to Beds 2 and 3 of the Plenus Marl (Fig. 1), based on a positive excursion in carbonate oxygen isotopes.

The PCE interval is characterized by a 3–7°C cooling of sea surface temperatures in the proto-North Atlantic and the European shelf (e.g., Forster et al., 2007; Sinninghe Damsté et al., 2010; van Helmond et al., 2014a; 2015). In several regions, such as the Western Interior Seaway (Eldrett et al., 2014) and proto-North Atlantic (e.g., Forster et al., 2007), the stratigraphic position of the PCE is characterized by minima in sediment organic carbon content and redox-sensitive element concentrations, which indicates improved oxygenation of bottom waters (e.g., van Helmond et al., 2014b). Furthermore the stratigraphic position of the PCE coincides with a decline in atmospheric $p\text{CO}_2$ (e.g., Kuypers et al., 1999; Sinninghe Damsté et al., 2008; Barclay et al., 2010), which is thought to be a consequence of enhanced sequestration of organic carbon in sediments during the early stages of OAE2 (e.g., Barclay et al., 2010; Sinninghe Damsté et al., 2010). The incursion of Boreal fauna into lower latitudes has only been documented for the European shelf. A causal relation between $p\text{CO}_2$ drawdown, sea surface cooling, bottom water oxygenation and the PCE has been proposed (e.g., Forster et al., 2007; Sinninghe Damsté et al., 2010; Jarvis et al., 2011; van Helmond, 2014b).

Previously, it remained unclear whether the migration of Boreal fauna was related to a migration of multiple components of marine food webs. Recently, van Helmond et al. (2014a, 2015) showed that the first consistent presence (FCP; presence of multiple specimens in consecutive samples) of dinoflagellate cysts (dinocysts) belonging to the *Cyclonephelium compactum-membraniphorum* morphological plexus (*Ccm*; see below for a detailed discussion on taxonomic status) in two sections on the proto-North Atlantic and European shelf coincided with a cooling of sea surface temperatures at the stratigraphic level of the PCE. To test whether *Ccm* was truly a high latitude taxon and if widespread migration of these dinoflagellates occurred during the PCE, we studied a high-latitude site



in northwest Alberta, Canada (Pratts Landing) and compiled a global distribution of *Ccm* across OAE2, calibrated using biostratigraphy and carbon isotope stratigraphy.

2. Materials and methods

2.1 The Pratts Landing section

5 Pratts Landing is an outcrop locality in the Peace River valley in northwest Alberta, Canada (56°01'14"N, 118°48'47"W). During the Late Cretaceous, the study site was located at ~61°N, ±5 (van Hinsbergen et al., 2015; paleolatitude.org), on the eastern flank of the foredeep basin, about 160 km from the contemporaneous shoreline of the Western Interior Seaway (Fig. 2; Varban and Plint, 2008). The studied section of predominantly thinly bedded silt- and claystones spans about 23 m of upper
10 Cenomanian to lower Turonian strata, based on stable carbon isotope stratigraphy and inoceramid biostratigraphy (Fig. 3).

2.2 Stable isotope geochemistry

The carbon isotope composition of bulk organic carbon ($\delta^{13}\text{C}_{\text{org}}$) was measured at 20 cm intervals across OAE2 in order to constrain its exact position, and at 50 cm intervals for the remainder of the
15 section. Analyses were performed in the Stable-Isotope Biogeochemistry Laboratory of the School of Geography and Earth Sciences, McMaster University, Hamilton, Ontario, Canada. In total, 77 samples were treated with 3N HCl to remove carbonates, rinsed with demineralised water, freeze-dried and powdered. Between 1 and 3 mg of powdered sediment sample was weighed in tin capsules, and put in a rotating carousel for subsequent combustion in an elemental analyser. After purification of the gas
20 sample it was passed through a SIRA II Series 2 dual-inlet isotope-ratio mass-spectrometer to determine the stable carbon isotopic composition of organic matter. Carbon isotope ratios were measured against an international standard, NBS-21. The analytical reproducibility, based on replicate samples, was better than 0.1‰.

2.3 Palynological processing

25 Dinocyst abundances were determined for 21 samples, covering the entire section, using standard palynological methods. About 5 grams of freeze-dried sediment was processed following a standardized quantitative method (e.g., Sluijs et al., 2003), which involves the addition of a known amount of *Lycopodium* marker spores (Stockmar, 1971). To dissolve carbonates and silicates, HCl (~30%) and HF (~38%) were added, respectively. After centrifugation, acids were discarded. The
30 remaining residues were sieved over a 15 μm nylon mesh and the >15 μm fraction was mounted on slides for analysis by light microscopy. Samples were counted to a minimum of 250 dinocysts, which were identified to genus, or species level at 500x magnification, following the taxonomy of Fensome and Williams (2004). All samples and slides are stored in the collection of the Laboratory of



Palaeobotany and Palynology, Utrecht University, the Netherlands. All data ($\delta^{13}\text{C}_{\text{org}}$ and palynology) are listed in a supplementary file (Table S1).

2.4 Taxonomy and literature survey

Originally the cysts *Cyclonephelium membraniphorum* (Cookson and Eisenack, 1962), which was
5 renamed *Cauverodinium membraniphorum* (Masure in Fauconnier and Masure, 2004), were
differentiated from *C. compactum* (Deflandre and Cookson, 1955), based on the generally higher and
structurally ordered crests and membranes of *C. membraniphorum*. Additionally, cysts of *C.*
membraniphorum form a series of funnel-shaped structures bordering unornamented mid-dorsal and
mid-ventral areas. However, the apparent morphological variation regarding ornamentation within the
10 two species exceeds the defined difference between the two species. Therefore it was proposed to refer
to the dinocyst morphological complex *Cyclonephelium compactum-membraniphorum*, rather than
separating both species (Marshall and Batten, 1988). We agree that the two species are members of a
morphological continuum and therefore group all these morphotypes of this continuum from our study
site and the literature under the *Cyclonephelium compactum-membraniphorum* morphological plexus
15 (*Ccm*) (Fig. 4; Table 1). For the compilation of the global biogeographical distribution of *Ccm* prior to,
during and after OAE2, a literature survey was conducted.

3. Results and Discussion

3.1 Dinocyst biogeography

At Pratts Landing the OAE2 interval is recorded between 10.2 m and 16.8 m, based on a 2‰ positive
20 shift in $\delta^{13}\text{C}_{\text{org}}$ (Fig. 3). The Cenomanian-Turonian boundary is placed at 15.3 m, at the sharp base of a
20 cm thick, siltstone-rich and heavily gypsum-cemented mudstone lacking macrofauna. The base
Turonian marker species *Mytiloides puebloensis* was not found, but the succeeding Zone, characterized
by *M. goppelnensis* and *M. kossmati* starts approximately 25 cm above the basal surface (Fig. 3). *Ccm*
is a general constituent (1-4%) of the dinocyst assemblage at Pratts Landing throughout the section,
25 i.e., also below the onset of OAE2 (Fig. 3).

All localities (n=35) with reported cysts of *Ccm* (i.e. *Cauverodinium membraniphorum*,
Cyclonephelium membraniphorum, *Cyclonephelium compactum* and/or *Cyclonephelium compactum-*
membraniphorum) are listed in Table 1 and shown in Figure 5. The first common presence (FCP) of
Ccm could only be determined for 20 of the localities as a result of poor stratigraphic constraints and
30 only qualitative reporting of *Ccm*.

Recent dinocyst biostratigraphic studies from the East Coast Basin, New Zealand, show that the FCP
of *Ccm* was ca. 500 kyr before the onset of OAE2 (Schiöler and Crampton, 2014). At northern high
latitudes, notably Pratts Landing and the Norwegian Sea (Radmacher et al. 2015), *Ccm* is a consistent
constituent of the dinocyst assemblage throughout the late Cenomanian. In contrast, at most Northern
35 Hemisphere mid-latitude sites, *Ccm* has not been reported before OAE2, with the exception of a few
spot occurrences at Eastbourne and Iona-1 (Pearce et al., 2009; Eldrett et al., 2014). Crucially, *Ccm* was



never a consistent constituent of mid-latitude dinocyst assemblages before OAE2. This indicates that *Ccm* had a high-latitude biogeographical distribution in both hemispheres before OAE2.

Five Northern Hemisphere shelf sites in Europe and North America, namely Pratts Landing, Iona-1 (southwest Texas, USA), Bass River (New Jersey, USA), Eastbourne (East Sussex, UK) and Wunstorf (Lower Saxony, Germany), were selected to compare established biozonation, high-resolution records of $\delta^{13}\text{C}$, and the relative abundances of *Ccm* (Fig. 6; Pearce et al., 2009; Eldrett et al., 2014; van Helmond et al., 2014a; 2015). Maximum relative abundances of *Ccm* (i.e., >10%) are recorded during the first maximum in the OAE2 characterizing carbon isotope excursion (point “A” — cf. Voigt et al., 2008), at Pratts Landing (Figs. 3, 6). At the same stratigraphic position, *Ccm* becomes abundant at several other Northern Hemisphere mid-latitude sites, for example, the southern part of the Western Interior Seaway, the proto-North Atlantic shelf, the European shelf, and the Tethys (Figs. 5, 6; Table 1). Despite a spot occurrence at point “A”, the FCP of *Ccm* seems somewhat delayed at Eastbourne (i.e., Plenus Marl Bed 7 – Fig. 6; Pearce et al., 2009), this is a local phenomenon, because in other English Chalk sections (e.g., Dodsworth, 2000) the FCP of *Ccm* coincides with that of other Northern Hemisphere mid-latitude sites.

3.2 Ecology

At Bass River and Wunstorf the FCP of *Ccm* precisely correlates with a drop in sea surface temperature (van Helmond et al., 2014a; 2015), leading to the suggestion that the dinoflagellate taxon that produced *Ccm* migrated to these sites in response to climatic cooling. We therefore suggest that sea surface temperature was the primary control on the biogeographical distribution of *Ccm* outside high latitude regions. For the Shell Iona-1 core the FCP of *Ccm* coincides with a minimum in organic carbon, redox-sensitive elements and relatively high abundances of benthic foraminifera and trace fossils indicative of a period of improved oxygenation of bottom waters (Eldrett et al., 2014). This is in agreement with previous observations for the interval showing PCE-related cooling of sea surface temperature in the proto-North Atlantic (Forster et al., 2007; Sinninghe Damsté et al., 2010; van Helmond et al., 2014b). The sustained presence of *Ccm* after the PCE at all sites, except Bass River (Fig. 6), suggests that, in addition to sea surface temperature, other environmental and paleoceanographic factors became dominant in determining the distribution of *Ccm* once it had occupied niches at lower latitudes. For example, salinity and proximity to the shoreline may have been important (Harris and Tocher, 2003).

The migration of *Ccm* towards lower latitudes in response to cooling resembles dinoflagellate migration events during other periods of marked climatic change. Dinocysts referable to the Arctic Paleogene taxon *Svalbardella* were encountered in mid- and low-latitudes during the most pronounced Oligocene glaciations (ca. 30–25 Ma; van Simaey et al., 2005). In contrast, during the Paleocene–Eocene Thermal Maximum, tropical species of the dinocyst genus *Apectodinium* moved from low toward high latitudes in response to peak warmth (Crouch et al., 2003; Sluijs et al., 2007). Studies across the Cretaceous–Paleogene boundary indicate initial high latitude to equatorial dinoflagellate migration at the boundary, followed by a reverse migration. This presumably took place in response to



impact-related initial climatic cooling followed by a return to warmer conditions (Brinkhuis et al., 1998; Galeotti et al., 2004; Vellekoop et al., 2014).

The biogeographical expansion of *Ccm* towards the equator seems to be a relatively strong response to a moderate change in sea surface temperature (ca. 3–5°C). The southward migration of *Ccm* over
5 relatively large distances, i.e. 20°–30° of latitude southwards, may have been amplified by the flatter meridional temperature gradients across OAE2 (e.g., Sinninghe Damsté et al., 2010). Compared to the present day, which is characterized by a much steeper meridional temperature gradient, relatively small changes in temperature in the mid-Cretaceous and early Paleogene may have had a much larger impact on the distribution of marine organisms.

10 3.3 A new stratigraphic marker

Most of the Cretaceous is covered by the Normal Superchron C34n (ca. 126–84 Ma; Gradstein et al., 2012), hampering application of magnetostratigraphy. Stratigraphic correlation for the Cenomanian–
Turonian boundary interval therefore relies on biostratigraphy and carbon isotope stratigraphy (Gale et al., 2005) as well as on recent advances in astrochronology (e.g., Meyers et al., 2012; Eldrett et al.,
15 2015). Pelagic sediments are often carbonate-poor, because the calcite compensation depth was relatively shallow during OAE2, complicating planktonic foraminifer and calcareous nannofossil biostratigraphy (e.g., Erba, 2004). Consequently, carbon isotope stratigraphy is the main stratigraphic tool for OAE2 because the positive carbon isotope excursion is recognized in all active carbon reservoirs (Tsikos et al., 2004). Calibration of carbon isotope stratigraphy with bioevents is, however,
20 essential to establish detailed stratigraphic frameworks.

The coincidence of the FCP of *Ccm* with the base of the *W. archaeocretacea* and the upper part of the *M. geslinianum* zone close to the first maximum in the positive carbon isotope excursion (point “A”; Fig. 6), suggests that dinoflagellate migration probably occurred within thousands to ten thousand years. The FCP of *Ccm* thus represents a useful biostratigraphic marker, being, to date, the only widely
25 found microfossil to mark the PCE, except at high latitudes.

4. Conclusions

A global compilation of dinocyst assemblage records combined with new data from a high-latitude site spanning OAE2 illustrates the migration of dinoflagellates, that produced the dinocyst morphological complex *Ccm*, from high-latitudes to mid-latitudes during the early stages of OAE2 (latest
30 Cenomanian). The first consistent presence of this taxon at mid-latitudes correlates with the stratigraphic position of the Plenus Cold Event, following its original definition by Gale and Christensen (1996), making it the sole widely found microfossil to mark this cold spell. The coincidence of the first consistent presence of *Ccm* in the mid-latitudes with this transient cooling, implies lasting reorganization of phytoplankton biogeography in response to rapid climate change
35 during the Late Cretaceous supergreenhouse. The migration of *Ccm* in response to climatic cooling resembles previously recognized dinoflagellate migration events during comparable periods of transient climate change, e.g., the Oligocene glaciations and the Paleocene–Eocene Thermal Maximum.



Author contributions

N. van Helmond, A. Sluijs and H. Brinkhuis designed the research. Samples of the Pratts Landing section were collected in the field by G. Plint, I. Walaszczyk and D. Gröcke. Palynological analyses were carried out by N. van Helmond, N. Papadomanolaki and B. van de Schootbrugge. Carbon isotope stratigraphy was carried out by D. Gröcke, G. Plint and J. Trabucho-Alexandre. Inoceramid biostratigraphy was carried out by I. Walaszczyk. Compilation of the global biogeographical distribution of *Cem* was carried out by N. van Helmond, H. Brinkhuis, M. Pearce and J. Eldrett. N. van Helmond and A. Sluijs prepared the manuscript with input from all authors.

Acknowledgements

This paper used data generated on sediments recovered and curated by the International Ocean Discovery Program. We thank J. van Tongeren and N. Welters for laboratory assistance. Utrecht University supported this research with a “Focus en Massa” program grant to H. Brinkhuis. Statoil provided additional financial support. The European Research Council (ERC) under the European Union’s Seventh Framework Program provided funding for this work by ERC Starting Grant 259627 to A. Sluijs. Regional studies of Cretaceous strata in western Canada were supported by a Natural Sciences and Engineering Research Council of Canada (NSERC) Discovery Grant to A.G. Plint. Darren R. Gröcke acknowledges funding by a UK Natural Environment Research Council (NERC) Standard Grant (NE/H021868/1). This work was carried out under the program of the Netherlands Earth System Science Centre (NESSC).

References

- Barclay, R.S., McElwain, J.C., and Sageman, B.B.: Carbon sequestration activated by a volcanic CO₂ pulse during Oceanic Anoxic Event 2, *Nat. Geosci.*, 3, 205–208, doi:10.1038/NGEO757, 2010.
- Bowman, A.R., and Bralower, T.J.: Paleoceanographic significance of high-resolution carbon isotope records across the Cenomanian–Turonian boundary in the Western Interior and New Jersey coastal plain, USA, *Mar. Geol.*, 217, 305–321, doi:10.1016/j.margeo.2005.02.010, 2005.
- Brinkhuis, H., Bujak, J.P., Smit, J., Versteegh, G.J.M., and Visscher, H.: Dinoflagellate-based sea surface temperature reconstructions across the Cretaceous–Tertiary boundary, *Palaeogeogr. Palaeoclimatol.*, 141, 67–83, doi:10.1016/S0031-0182(98)00004-2, 1998.
- Čech, S., Hradecká, L., Svobodová, M., and Švábenická, L.: Cenomanian and Cenomanian–Turonian boundary in the southern part of the Bohemian Cretaceous Basin, Czech Republic, *Bull. Geosci.*, 80, 321–354, 2005.
- Cookson, I.C., and Eisenack, A.: Additional microplankton from Australian Cretaceous sediments, *Micropaleontology*, 8, 485–507, 1962.
- Courtinat, B., Crumière, J. P., Méon, H., and Schaaf, A.: Les associations de kystes de dinoflagellés du Cénomaniens–Turonien de Vergons (Bassin Vocontien France), *Geobios-Lyon*, 24, 649–666, doi:10.1016/S0016-6995(06)80293-7, 1991.



- Crampton, J.S., Raine, I., Strong, C.P., and Wilson, G.J.: Integrated biostratigraphy of the Raukumara Series stratotype (Cenomanian to Coniacian) at Mangaotane Stream, Raukumara Peninsula, New Zealand, *New Zeal. J. Geol. Geop.*, 44, 365-389, doi:10.1080/00288306.2001.9514945, 2001.
- 5 Crouch, E.M., Dickens, G.R., Brinkhuis, H., Aubry, M.-P., Hollis, C.J., Rogers, K.M., and Visscher, H.: The Apectodinium acme and terrestrial discharge during the Paleocene Eocene thermal maximum: New palynological, geochemical and calcareous nannoplankton observations at Tawanui, New Zealand, *Palaeogeogr. Palaeoclimatol.*, 194, 387-403, doi:10.1016/S0031-0182(03)00334-1, 2003.
- 10 Deflandre, G., and Cookson, I.C.: Fossil microplankton from Australian late Mesozoic and Tertiary sediments, *Mar. Freshwater Res.*, 6, 242-314, 1955.
- Dodsworth, P.: Stratigraphy, microfossils and depositional environments of the lowermost part of the Welton Chalk Formation, late Cenomanian to early Turonian (Cretaceous) in eastern England: *P. York. Geol. Soc.*, 51, 45-64, doi:10.1144/pygs.51.1.45, 1996.
- 15 Dodsworth, P.: Trans-Atlantic dinoflagellate cyst stratigraphy across the Cenomanian-Turonian (Cretaceous) Stage boundary, *J. Micropalaeontol.*, 19, 69-84, doi:10.1144/jm.19.1.69, 2000.
- Dodsworth, P.: The distribution of dinoflagellate cysts across a Late Cenomanian carbon isotope ($\delta^{13}\text{C}$) anomaly in the Pulawy borehole, central Poland, *J. of Micropalaeontol.*, 23, 77-80, doi:10.1144/jm.23.1.77, 2004a.
- 20 Dodsworth, P.: The palynology of the Cenomanian-Turonian (Cretaceous) boundary succession at Aksudere in Crimea, Ukraine, *Palynology*, 28, 129-141, doi:10.1080/01916122.2004.9989594, 2004b.
- Du Vivier, A.D.C., Selby, D., Sageman, B.B., Jarvis, I., Gröcke, D.R., and Voigt, S.: Marine $^{187}\text{Os}/^{188}\text{Os}$ isotope stratigraphy reveals the interaction of volcanism and ocean circulation during Oceanic Anoxic Event 2, *Earth Planet. Sc. Lett.*, 389, 23-33, doi:10.1016/j.epsl.2013.12.024, 2014.
- 25 Eldrett, J.S., Minisini, D., and Bergman, S.C.: Decoupling of the carbon cycle during Ocean Anoxic Event 2, *Geology*, 42, 567-570, doi:10.1130/G35520.1, 2014.
- Eldrett, J.S., Ma, C., Bergman, S.C., Lutz, B., Gregory, J., Dodsworth, P., Phipps, M., Hardas, P., Minisini, D., Ozkan, A., Ramezani, J., Bowring, S., Kamo, S., Ferguson, K., MacAulay, C., and Kelly, A.: An astronomically calibrated stratigraphy of the Cenomanian-Turonian Eagle Ford Formation, Texas, USA: implications for global chronostratigraphy, *Cretaceous Res.*, 56, 316-344, doi:10.1016/j.cretres.2015.04.010, 2015.
- 30 Erba, E.: Calcareous nannofossils and Mesozoic oceanic anoxic events, *Mar. Micropaleontology*, 52, 85-106, doi:10.1016/j.marmicro.2004.04.007, 2004.
- Fauconnier, D. and Masure, E.: Les dinoflagellés fossiles: guide pratique de détermination: les genres à processus et à archéopyle apical. Editions BRGM, Collection Scientifique, Orléans, France, 600 pp, 2004.
- 35 Fensome, R.A., and Williams, G.L.: The Lentin and Williams Index of Fossil Dinoflagellates, 2004 Edition, volume 42, American Association of Stratigraphic Palynologists Contribution Series, Dallas, Texas, USA, 909 pp., 2004.



- Forster, A., Schouten, S., Moriya, K., Wilson, P.A., and Sinninghe Damsté, J.S.: Tropical warming and intermittent cooling during the Cenomanian/Turonian oceanic anoxic event 2: sea-surface temperature records from the equatorial Atlantic, *Palaeoceanography*, 22, PA1219, doi:10.1029/2006PA001349, 2007.
- 5 Gale, A.S., and Christensen, W.K.: Occurrence of the belemnite *Actinocamax plenus* in the Cenomanian of SE France and its significance, *Bull. Geol. Soc. Den.*, 43, 68–77, 1996.
- Gale, A.S., Kennedy, W.J., Voigt, S., and Walaszczyk, I.: Stratigraphy of the Upper Cenomanian–Lower Turonian Chalk succession at Eastbourne, Sussex, UK: ammonites, inoceramid bivalves and stable carbon isotopes, *Cretaceous Res.*, 26, 460–487, doi:10.1016/j.cretres.2005.01.006, 2005.
- 10 Galeotti, S., Brinkhuis, H., and Huber, M.: Records of post–Cretaceous-Tertiary boundary millennial-scale cooling from the western Tethys: A smoking gun for the impact-winter hypothesis?, *Geology* 32, 529–532, doi: 10.1130/G20439.1, 2004.
- Gradstein F.M., Ogg J.G., Schmitz M.D., and Ogg G.M.: *The Geologic Time Scale 2012*, Elsevier, Oxford (UK), 1144 pp., 2012.
- 15 Harris, A.J., and Tocher, B.A.: Palaeoenvironmental analysis of Late Cretaceous dinoflagellate cyst assemblages using high-resolution sample correlation from the Western Interior Basin, USA, *Mar. Micropaleontology*, 48, 127–148, doi:10.1016/S0377-8398(03)00002-1, 2003.
- Hasegawa, T., Crampton, J.S., Schiøler, P., Field, B., Fukushi, K., and Kakizaki, Y.: Carbon isotope stratigraphy and depositional oxia through Cenomanian/Turonian boundary sequences (Upper
 20 Cretaceous) in New Zealand, *Cretaceous Res.*, 40, 61–80, doi:10.1016/j.cretres.2012.05.008, 2013.
- Huber, B.T., Norris, R.D., and MacLeod, K.G.: Deep-sea paleotemperature record of extreme warmth during the Cretaceous, *Geology*, 30, 123–126, doi: 10.1130/0091-7613(2002)030<0123:DSPROE>2.0.CO;2, 2002
- 25 Jarvis, I., Carson, G.A., Cooper, M.K.E., Hart, M.B., Leary, P.N., Tocher, B.A., Horne, D., and Rosenfeld, A.: Microfossil assemblages and the Cenomanian–Turonian (Late Cretaceous) oceanic anoxic event, *Cretaceous Res.*, 9, 3–103, doi:10.1016/0195-6671(88)90003-1, 1998.
- Jarvis, I., Lignum, J.S., Gröcke, D.R., Jenkyns, H.C., and Pearce, M.A.: Black shale deposition, atmospheric CO₂ drawdown, and cooling during the Cenomanian–Turonian Oceanic Anoxic Event,
 30 *Paleoceanography*, 26, PA3201, doi:10.1029/2010PA002081, 2011.
- Jefferies, R.P.S.: The stratigraphy of the *Actinocamax plenus* Subzone (Turonian) in the Anglo-Paris Basin, *P. of the Geologist. Assoc.*, 74, 1–33, 1963.
- Jenkyns, H.C.: Geochemistry of oceanic anoxic events, *Geochem., Geophys., Geosy.*, 11, Q03004, doi:10.1029/2009GC002788, 2010.
- 35 Jenkyns, H.C., Forster, A., Schouten, S., and Sinninghe Damsté, J.S.: High temperatures in the late Cretaceous Arctic Ocean, *Nature*, 432, 888–892, doi:10.1038/nature03143, 2004.
- Kuypers, M.M.M., Pancost, R.D., and Sinninghe Damsté, J.S.: A large and abrupt fall in atmospheric CO₂ concentration during Cretaceous times, *Nature*, 399, 342–345, 1999.



- Lamolda, M.A., and Mao, S.: The Cenomanian–Turonian boundary event and dinocyst record at Genuza (northern Spain), *Palaeogeogr. Palaeoclimatol.*, 150, 65–82, doi:10.1016/S0031-0182(99)00008-5, 1999.
- Li, H., and Habib, D.: Dinoflagellate stratigraphy and its response to sea level change in Cenomanian–Turonian sections of the Western Interior of the United States, *Palaaios*, 11, 15–30, 1996
- 5 Lignum, J.S.: Cenomanian (upper Cretaceous) palynology and chemostratigraphy: Dinoflagellate cysts as indicators of palaeoenvironmental and sea-level change, Ph.D thesis, Kingston University London, Kingston upon Thames, UK, 582 pp., 2009.
- Marshall, K.L., and Batten, D.J.: Dinoflagellate cyst associations in Cenomanian–Turonian “black shale” sequences of northern Europe, *Rev. Palaeobot. Palynol.*, 54, 85–103, doi:10.1016/0034-6667(88)90006-1, 1988.
- 10 Meyers, S.R., Sageman, B.B., and Arthur, M.A.: Obliquity forcing and the amplification of high-latitude climate processes during Oceanic Anoxic Event 2, *Paleoceanography*, 27, PA3212, doi:10.1029/2012PA002286, 2012.
- 15 McMinn, A.: Outline of a Late Cretaceous dinoflagellate zonation of northern Australia, *Alcheringa*, 12, 137–156, 1988.
- Mohr, B.A., Wähnert, V., and Lazarus, D.: Mid-Cretaceous paleobotany and palynology of the central Kerguelen Plateau, Southern Indian Ocean (ODP leg 183, site 1138), volume 183, Frey, F.A., Coffin, M.F., Wallace, P.J., and Quilty, P.G. (Eds.), *Proc. ODP: Sci. Results*, College Station, Texas, Ocean Drilling Program, 1–39, 2002.
- 20 Paul, C.R.C., Lamolda, M.A., Mitchell, S.F., Vaziri, M.R., Gorostidi, A. and Marshall, J.D: The Cenomanian/Turonian boundary at Eastbourne (Sussex, UK): a proposed European reference section, *Palaeogeogr. Palaeoclimatol.*, 150, 83–121, doi:10.1016/S0031-0182(99)00009-7, 1999.
- Pavlishina, P., and Wagreich, M.: Biostratigraphy and paleoenvironments in a northwestern Tethyan Cenomanian–Turonian boundary section (Austria) based on palynology and calcareous nannofossils, *Cretaceous Res.*, 38, 103–112, doi:10.1016/j.cretres.2012.02.005, 2012.
- 25 Pearce, M.A., Jarvis, I., and Tocher, B.A.: The Cenomanian–Turonian boundary event, OAE 2 and palaeoenvironmental change in epicontinental seas: new insights from the dinocyst and geochemical records, *Palaeogeogr. Palaeoclimatol.*, 280, 207–234, doi:10.1016/j.palaeo.2009.06.012, 2009.
- 30 Peyrot, D., Barroso-Barcenilla, F., Barrón, E., and Comas-Rengifo, M.J.: Palaeoenvironmental analysis of Cenomanian–Turonian dinocyst assemblages from the Castilian Platform (northern-Central Spain), *Cretaceous Res.*, 32, 504–526, doi:10.1016/j.cretres.2011.03.006, 2011.
- Peyrot, D., Barroso-Barcenilla, F., and Feist-Burkhardt, S.: Palaeoenvironmental controls on late Cenomanian–early Turonian dinoflagellate cyst assemblages from Condemios (Central Spain), *Rev. Palaeobot. Palynol.*, 180, 25–40, doi:10.1016/j.revpalbo.2012.04.008, 2012.
- 35 Prauss, M.L.: The Cenomanian/Turonian Boundary Event (CTBE) at Wunstorf, north-west Germany, as reflected by marine palynology, *Cretaceous Res.*, 27, 872–886, doi:10.1016/j.cretres.2006.04.004, 2006.



- Radmacher, W., Mangerud, G., and Tyszka, J.: Dinoflagellate cyst biostratigraphy of Upper Cretaceous strata from two wells in the Norwegian Sea, *Rev. Palaeobot. Palyno.*, 216, 18–32, doi:10.1016/j.revpalbo.2014.12.007, 2015.
- Schiøler, P., and Crampton, J.S.: Dinoflagellate biostratigraphy of the Arowhanan Stage (upper
 5 Cenomanian–lower Turonian) in the East Coast Basin, New Zealand, *Cretaceous Res.*, 48, 205–224, doi:10.1016/j.cretres.2013.11.011, 2014.
- Schlanger, S.O., and Jenkyns, H.C.: Cretaceous Oceanic Anoxic Events: causes and consequences, *Geol. Mijnbouw*, 55, 179–184, 1976.
- Scotese, C.R.: Atlas of Earth History, volume 1, PALEOMAP Project, Arlington, Texas, USA, 2001.
- 10 Sinninghe Damsté, J.S., Kuypers, M.M.M., Pancost, R.D., and Schouten, S.: The carbon isotopic response of algae, (cyano)bacteria, archaea and higher plants to the late Cenomanian perturbation of the global carbon cycle: Insights from biomarkers in black shales from the Cape Verde Basin (DSDP Site 367), *Org. Geochem.*, 39, 1703–1718, doi:10.1016/j.orggeochem.2008.01.012, 2008.
- Sinninghe Damsté, J.S., van Bentum, E.C., Reichart, G.J., Pross, J., and Schouten, S.: A CO₂ decrease-
 15 driven cooling and increased latitudinal temperature gradient during the mid-Cretaceous Oceanic Anoxic Event 2, *Earth Planet. Sc. Lett.*, 293, 97–103, doi:10.1016/j.epsl.2010.02.027, 2010.
- Sluijs, A., Brinkhuis, H., Stickley, C.E., Warnaar, J., Williams, G.L., and Fuller, M.: Dinoflagellate cysts from the Eocene–Oligocene transition in the Southern Ocean: Results from ODP Leg 189, volume 189, Exxon, N.F., et al. (Eds.), *Proc. ODP: Sci Results*, College Station, Texas, Ocean
 20 Drilling Program, 1–42, 2003.
- Sluijs, A., Bowen, G.J., Brinkhuis, H., Lourens, L.J., and Thomas, E.: The Palaeocene-Eocene thermal maximum super greenhouse: Biotic and geochemical signatures, age models and mechanisms of global change, in: Deep time perspectives on climate change: Marrying the signal from computer models and biological proxies, Williams, M., et al. (Eds.), *Micropalaeontological Society Special
 25 Publication 2*, Geological Society London, London, UK, 323–349, 2007.
- Stockmarr, J.: Tablets with spores used in absolute pollen analysis, *Pollen et Spores*, 13, 615–621, 1971.
- Tocher, B. A., and Jarvis, I.: Dinocyst distributions and stratigraphy of two Cenomanian–Turonian
 30 boundary (Upper Cretaceous) sections from the western Anglo-Paris Basin, *J. Micropalaeontology*, 14, 97–105, doi: 10.1144/jm.14.2.97, 1995.
- Tsikos, H., Jenkyns, H.C., Walsworth-Bell, B., Petrizzo, M.R., Forster, A., Kolonic, S., Erba, E., Premoli Silva, I., Baas, M., Wagner, T., and Sinninghe Damsté, J.S.: Carbon-isotope stratigraphy recorded by the Cenomanian–Turonian Oceanic Anoxic Event: correlation and implications based on three key localities, *J. Geol. Soc. London*, 161, 711–719, doi: 10.1144/0016-764903-077, 2004.
- 35 Van Helmond, N.A.G.M., Sluijs, A., Reichart, G.J., Sinninghe Damsté, J.S., Slomp, C.P., and Brinkhuis, H.: A perturbed hydrological cycle during Oceanic Anoxic Event 2, *Geology*, 42, 123–126, doi: 10.1130/G34929.1, 2014a.
- Van Helmond, N.A.G.M., Ruvalcaba Baroni, I., Sluijs, A., Sinninghe Damsté, J.S., and Slomp C.P.: Spatial extent and degree of oxygen depletion in the deep proto-North Atlantic basin during



- Oceanic Anoxic Event 2, *Geochem., Geophys., Geosy.*, 15, 4254–4266, doi:10.1002/2014GC005528, 2014b
- Van Helmond, N.A.G.M., Sluijs, A., Sinninghe Damsté, J.S., Reichert, G.-J., Voigt, S., Erbacher, J., Pross, J., and Brinkhuis, H.: Freshwater discharge controlled deposition of Cenomanian-Turonian black shales on the NW European epicontinental shelf (Wunstorf, North Germany), *Clim. Past*, v. 11, 495–508, doi:10.5194/cp-11-495-2015, 2015
- Van Hinsbergen, D.J.J., de Groot, L.V., van Schaik, S.J., Spakman, W., Bijl, P.K., Sluijs, A., Langereis, C.G., and Brinkhuis, H.: A Paleolatitude Calculator for Paleoclimate Studies, *PloS one*, v. 10, e0126946, doi:10.1371/journal.pone.0126946, 2015.
- 10 Van Simaey, S., Brinkhuis, H., Pross, J., Williams, G.L., and Zachos, J.C.: Arctic dinoflagellate migrations mark the strongest Oligocene glaciations, *Geology*, 33, 709–712, doi: 10.1130/G21634.1, 2015.
- Varban, B.L., and Plint, A.G.: Palaeoenvironments, palaeogeography, and physiography of a large, shallow, muddy ramp: Late Cenomanian-Turonian Kaskapau Formation, Western Canada foreland basin, *Sedimentology*, 55, 201–233, doi:10.1111/j.1365-3091.2007.00902.x, 2008.
- 15 Vellekoop, J., Sluijs, A., Smit, J., Schouten, S., Weijers, J.W.H., Sinninghe Damsté, J. S., and Brinkhuis, H.: Rapid short-term cooling following the Chicxulub impact at the Cretaceous–Paleogene boundary, *P. Natl. Acad. Sci. USA*, 111, 7537–7541, doi:10.1073/pnas.1319253111, 2014.
- 20 Voigt, S., Gale, A.S., and Flögel, S.: Midlatitude shelf seas in the Cenomanian-Turonian greenhouse world: Temperature evolution and North Atlantic circulation, *Paleoceanography*, 19, PA4020, doi:10.1029/2004PA001015, 2004.
- Voigt, S., Gale, A.S., and Voigt, T.: Sea-level change, carbon cycling and palaeoclimate during the Late Cenomanian of northwest Europe; an integrated palaeoenvironmental analysis: *Cretaceous Res.*, 27, 836–858, doi:10.1016/j.cretres.2006.04.005, 2006.
- 25 Voigt, S., Erbacher, J., Mutterlose, J., Weiss, W., Westerhold, T., Wiese, F., Wilmsen, M., and Wonik, T.: The Cenomanian–Turonian of the Wunstorf section (north Germany): Global stratigraphic reference section and new orbital time scale for oceanic anoxic event 2, *Newsl. Stratigr.*, 43, 65–89, doi:10.1127/0078-0421/2008/0043-0065, 2008.

30

35



Table 1. Overview of the localities where cysts of *Cyclonephelium compactum-membraniphorum* morphological plexus (*Ccm*) have been reported across the Cenomanian-Turonian boundary interval. In the fourth and fifth column an “X” marks whether the first consistent presence (FCP) of *Ccm* was before OAE2 or if it was associated with the first maximum in the positive carbon isotopic excursion (CIE), point “A” cf. Voigt et al., 2008. Question marks indicate that the FCP could not be determined accurately, resulting from insufficient supporting information, e.g. high-resolution carbon isotope stratigraphy or unquantified abundances of *Ccm*. Localities further discussed in the article are in bold. Western Interior Seaway (WIS).

10

15

20

25

30

35

40



Site ID	Region	Locality	FCP of <i>Ccm</i> prior to OAE2	FCP of <i>Ccm</i> associated with CIE-“A”	References
<i>North America</i>					
1	WIS	Blue Point, Arizona, USA		X	Li and Habib, 1996; Harris and Tocher, 2003
a	WIS	Shell Iona-1, Texas, USA		X	Eldrett et al., 2014
2	WIS	Pueblo, Colorado, USA		X	Dodsworth, 2000; Harris and Tocher, 2003
3	WIS	Wahweap Wash, Utah, USA	?	?	Harris and Tocher, 2003
4	WIS	Bunker Hill, Kansas, USA	?	?	Harris and Tocher, 2003
5	WIS	Rebecca K. Bounds Core, Kansas, USA	?	?	Harris and Tocher, 2003
b	WIS	Pratts Landing, Alberta, Canada	X		this study
c	proto-N. Atlantic shelf	Bass River, New Jersey, USA		X	van Helmond et al., 2014a
<i>Europe</i>					
6	European shelf	Lulworth, Dorset, UK		X	Dodsworth, 2000
7	European shelf	Culver Cliff, Isle of Wight, UK		X	Lignum, 2009
8	European shelf	Folkstone, Kent, UK		X	Jarvis et al., 1988; Lignum, 2009
d	European shelf	Eastbourne, East-Sussex, UK		X	Pearce et al., 2009
9	European shelf	Eastern UK	?	?	Dodsworth, 1996
e	European shelf	Wunstorf, Lower Saxony, Germany		X	Marshall and Batten, 1988; Prauss, 2006; Lignum, 2009; van Helmond et al., 2015
10	European shelf	Misburg, Lower Saxony, Germany		X	Marshall and Batten, 1988
11	European shelf	Norwegian Sea, Norway	X		Radmacher et al., 2015
12	European shelf	Gröbern, Saxony Anhalt, Germany		X	Lignum, 2009
13	European shelf	Ratssteinbruch, Saxony, Germany		X	Lignum, 2009
14	European shelf	Pulawy, central Poland		X	Dodsworth, 2004a
15	European shelf	Nymburk, Central Bohemia, Czech Republic	?	?	Čech et al., 2005
16	European shelf	Aksudere, Crimea, Ukraine	?	?	Dodsworth, 2004b
17	European shelf	Bois du Gallet, St.-Sylvestre-de-Cormelles, Normandy, France	?	?	Tocher and Jarvis, 1995
18	European shelf	Les Fosses Blanches, Duneau, Maine, France	?	?	Tocher and Jarvis, 1995
19	European shelf	Ganuja, Castillian Platform, Spain	?	?	Lamolda and Mao, 1999
20	European shelf	Puentedey, Castillian Platform, Spain	?	?	Peyrot et al., 2011
21	European shelf	Fuentetoba, Castillian Plateau, Spain	?	?	Peyrot et al., 2011
22	European shelf	Tamajon, Castillian Plateau, Spain	?	?	Peyrot et al., 2011
23	European shelf	Condemos, Castillian Plateau, Spain	?	?	Peyrot et al., 2012
24	Tethys	Ultrahelvetic Rehkogelgraben, Austria	?	?	Pavlishina and Wagreich, 2012
25	Tethys	Pont d'Issole, Provence-Alpes-Côte d'Azur, France		X	Lignum, 2009
26	Tethys	Vergons, Provence-Alpes-Côte d'Azur, France		X	Courtinat et al., 1991; Lignum, 2009
<i>Southern Hemisphere</i>					
27	Southern Ocean	Central Kerguelen Plateau	?	?	Mohr et al., 2002
28	Indian Ocean	Northwestern Australia	X		McMinn, 1988
29	Pacific Ocean	East Coast Basin, New Zealand	X		Hasegawa et al., 2013; Schjoler and Crampton, 2014
30	Pacific Ocean	Mangaotane Stream, Raukumara Peninsula, New Zealand	X		Crampton et al., 2001

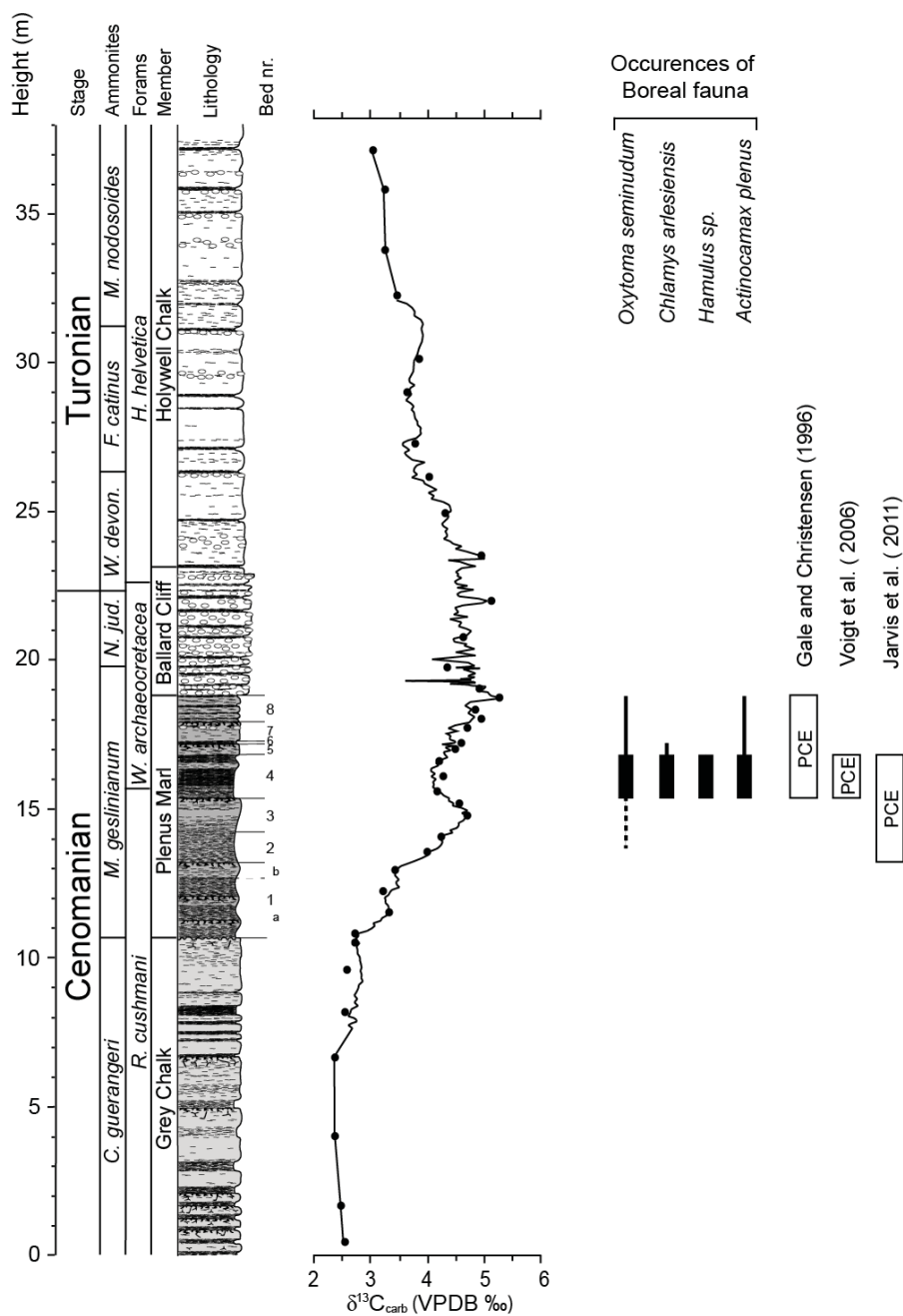


Figure 1. Biozonation, lithology, Plenus Marl beds (Jefferies, 1963) and $\delta^{13}C_{carb}$ (Pearce et al., 2009; high-resolution data derived from Paul et al., 1999) for the Cenomanian-Turonian boundary reference section at Eastbourne, combined with occurrences of Boreal fauna (Gale and Christensen, 1996). On the right side the ranges of the different definitions for the Plenus Cold Event are indicated.

5

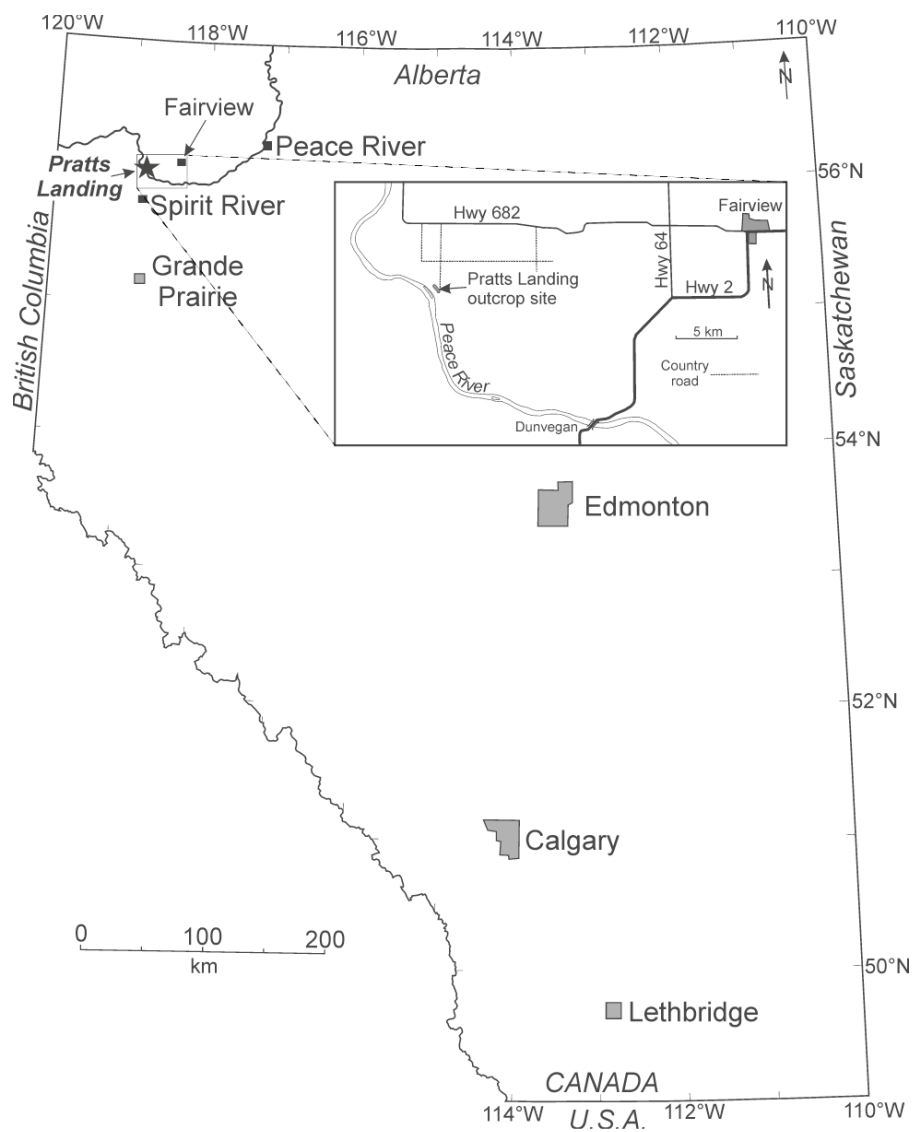


Figure 2. Map showing the southern part of Alberta. Study site at Pratts Landing is located on the Peace River about 70 km east of the Alberta-British Columbia border. Inset map shows details of the Peace River area in the vicinity of the town of Fairview, with the outcrop locality and access roads indicated.

5

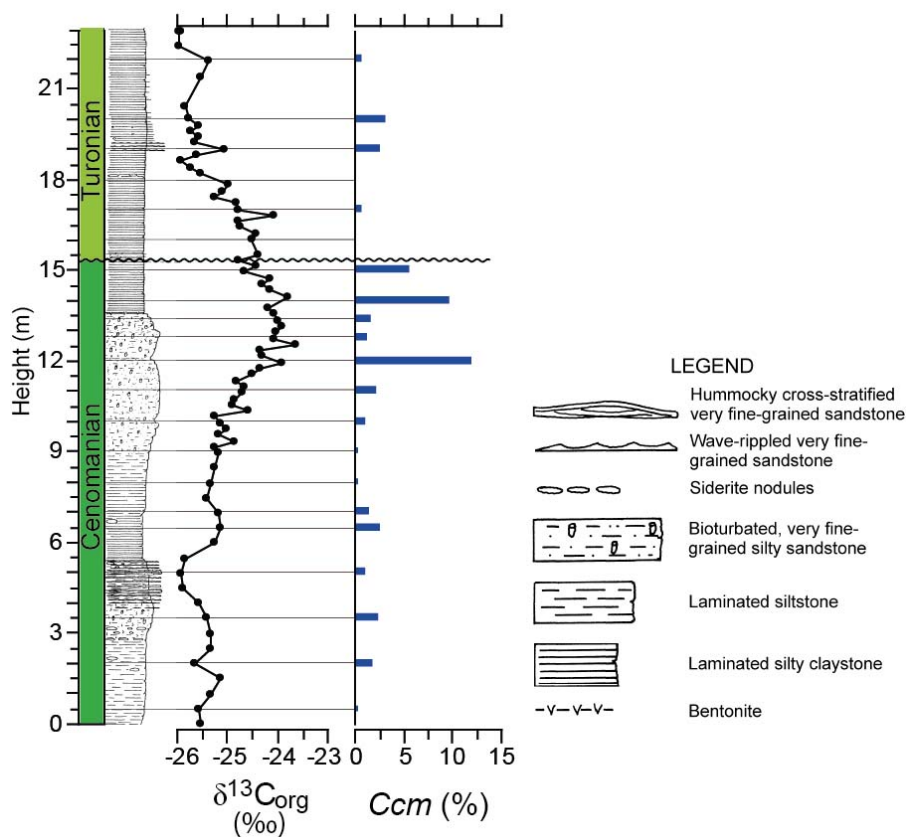


Figure 3. Lithology, $\delta^{13}\text{C}_{\text{org}}$ and abundances of *Cyclonephelium compactum-membraniphorum* morphological plexus (*Ccm*) for Pratts Landing. Sample intervals for palynology are indicated by horizontal black lines.

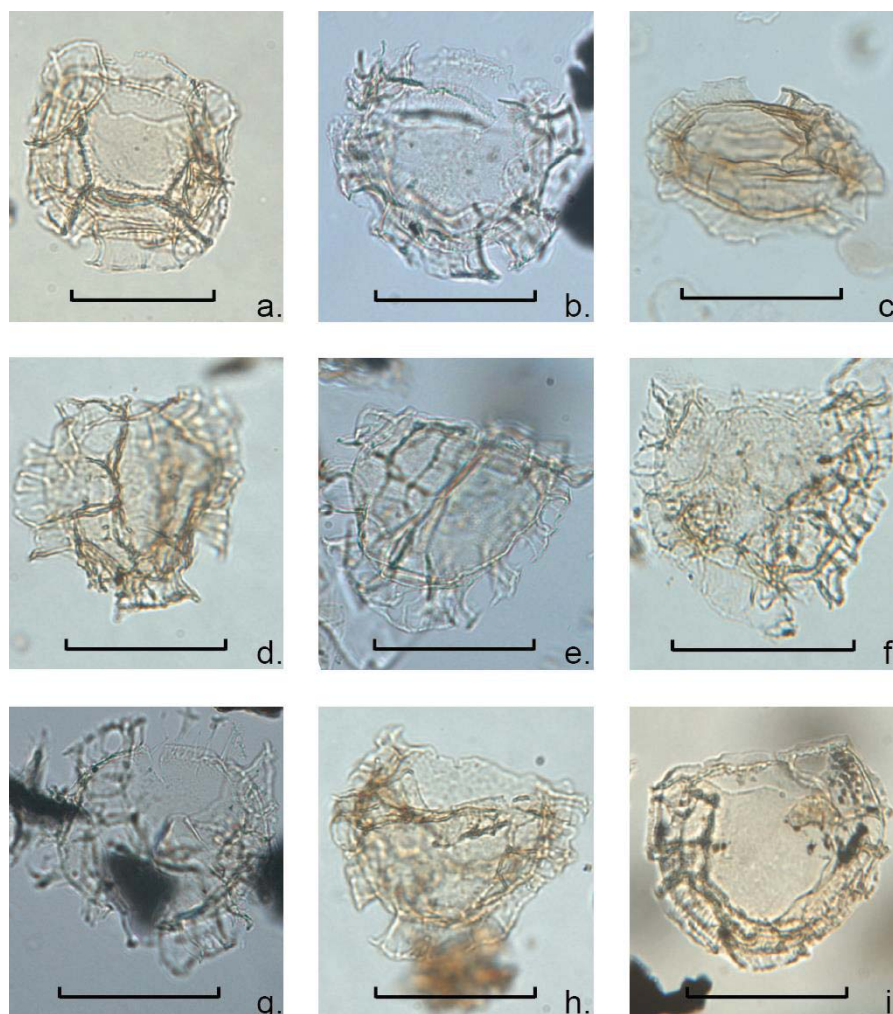
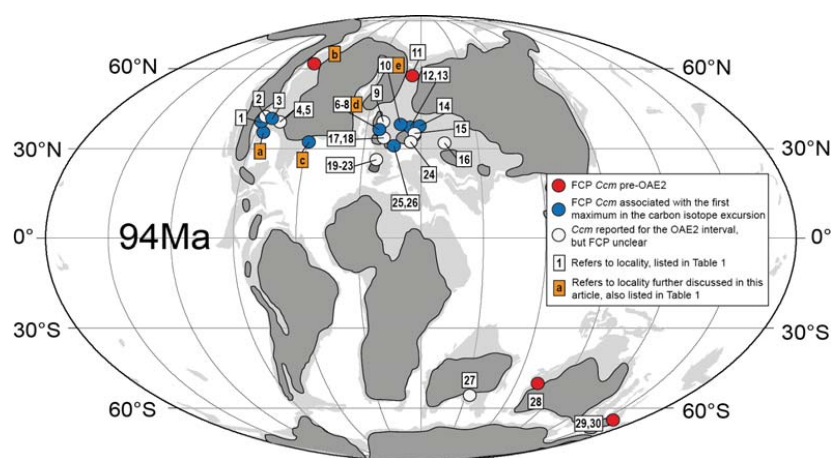


Figure 4. Various specimens of the *Cyclonephelium compactum-membraniphorum* morphological plexus (*Ccm*), gradually changing from the *C. membraniphorum* end-member (a-c) to the *C. compactum* end-member (g-i). Specimens a. (England Finder coordinates (EFc): U59/2-slide 1) and i. (EFc: L70/1-slide 2) are from Wunstorf sample 42.21 mbs, specimen b. (EFc: H13-slide 1) is from Bass River sample 590.69 mbs, specimen c. (EFc: R65/1-slide 1) is from Wunstorf sample 45.81 mbs, specimens d. (EFc: M59/2-slide 1) and h. (EFc: V53/2-slide 1) are from Pratts Landing sample 6.5 m, specimens e. (EFc: E59/2-slide 1) and g. (EFc: T64/3-slide 2) are from Bass River sample 590.08 mbs and specimen f. (EFc: J8/1-slide 1) is from Pratts Landing sample 12 m. Scale bars represent 50 μ m.

10



15 **Figure 5.** Compilation of the first consistent presence (FCP) of *Cyclonephelium compactum-membraniphorum* morphological plexus (*Ccm*) across Oceanic Anoxic Event 2. Numbers in white boxes refer to localities compiled in Table 1. Letters in orange boxes refer to the sites selected for comparison of established biozonation, high-resolution records of $\delta^{13}\text{C}$ and the relative abundances of *Ccm* (Fig. 6) also compiled in Table 1. The Mollweide projected paleogeographic map for the Cenomanian-Turonian boundary interval was generated at <http://www.odsn.de/odsn/services/paleomap/paleomap.html>. Continental plates are in light gray. Dry land in dark gray
20 after Scotese (2001).

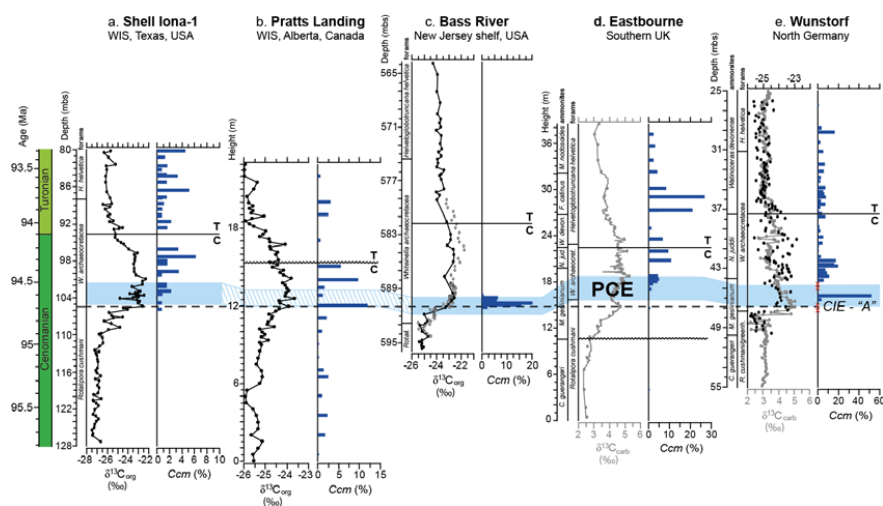


Figure 6. Overview of $\delta^{13}\text{C}_{\text{org}}$ and/or $\delta^{13}\text{C}_{\text{carb}}$, abundances of *Cyclonephelium compactum-membraniphorum* morphological plexus (*Ccm*) and foraminiferal and/or ammonite zonation for the studied sections; (a) Shell Iona-1 core (Eldrett et al., 2014); (b) Pratts Landing (this study); (c) Bass River (van Helmond et al., 2014a) open symbols is $\delta^{13}\text{C}_{\text{org}}$ derived from Bowman and Bralower (2005); (d) Eastbourne (Pearce et al., 2009), high-resolution $\delta^{13}\text{C}_{\text{carb}}$ data derived from Paul et al. (1999); (e) Wunstorf — relative abundances of *Ccm* from van Helmond et al. (2015), $\delta^{13}\text{C}_{\text{org}}$ from Du Vivier et al. (2014) and $\delta^{13}\text{C}_{\text{carb}}$ from Voigt et al. (2008), a red cross marks a barren sample. Age is from the astronomically tuned age model for the Shell Iona-1 core (Eldrett et al., 2015). Dashed line represents the first maximum in the carbon isotope excursion point “A” (cf. Voigt et al., 2008). Solid lines represent the Cenomanian–Turonian boundary. The blue shaded area represents the Plenus Cold Event according to its original definition (Gale and Christensen, 1996), the cooling in reconstructed sea surface temperatures at Bass River and Wunstorf (van Helmond et al., 2014a, 2015), and the (re)oxygenation of bottom waters in the Shell Iona-1 core (Eldrett et al., 2014). Note: the sections are plotted using different depth scales.